Supplementary information

S1 The width-averaged sediment concentration equation

Conservation of mass for the sediment is given by

$$\frac{\partial c}{\partial t} + \overrightarrow{\nabla} \cdot \overrightarrow{F} = 0 \tag{S.1}$$

here c is the $3D$ concentration, $\overrightarrow{F}$ is the total sediment flux which consists of an advective $\overrightarrow{F}_a$, settling $\overrightarrow{F}_s$ and diffusive $\overrightarrow{F}_d$ fluxes. They are given by

$$\overrightarrow{F}_a = c\overrightarrow{u} + cw\overrightarrow{e}_z,$$
$$\overrightarrow{F}_s = -cw_s\overrightarrow{e}_z,$$
$$\overrightarrow{F}_d = -K_h\overrightarrow{\nabla}c - K_v\frac{\partial c}{\partial z}\overrightarrow{e}_z.$$

where $\overrightarrow{u}$ is the horizontal velocity field, w the vertical velocity component, $\overrightarrow{e}_z$ the unit vector in z direction. K_h and K_v the horizontal and vertical eddy diffusivity coefficient, respectively.

Eq. (S.1) results in the sediment concentration equation

$$c_t + (uc)_x + (vc)_y + (c(w-w_s))_z = (K_h c_x)_x + (K_h c_y)_y + (K_v c_z)_z. \tag{S.2}$$

The width-integrated sediment concentration equation is obtained by integrating Eq. (S.2) over the width and using the Leibniz integral rule. It yields

$$\frac{\partial}{\partial t}\int_{B_2}^{B_1} c dy + \frac{\partial}{\partial x}\int_{B_2}^{B_1} ucdy + \frac{\partial}{\partial z}\int_{B_2}^{B_1} c(w-w_s)dy - \frac{\partial}{\partial x}\int_{B_2}^{B_1} K_h c_x dy - \frac{\partial}{\partial z}\int_{B_2}^{B_1} K_v c_z dy - \underbrace{\left[ucB_{1x} - vc - K_h c_x B_{1x} + K_h c_y\right]_{y=B_1}}_{1} + \underbrace{\left[ucB_{2x} - vc - K_h c_x B_{2x} + K_h c_y\right]_{y=B_2}}_{2} = 0. \tag{S.3}$$

Next we use the boundary conditions at the transversal sides of the estuary. The estuary is sketched in Fig. S.1. There is no flux through the side boundaries, i.e.

$$\overrightarrow{n}\cdot\left(c\overrightarrow{u} - K_h\overrightarrow{\nabla}c\right) = 0 \quad \text{at} \quad y = B_1(x) \text{ and } B_2(x), \tag{S.4}$$

where $\overrightarrow{n}_1$ is a normal outward pointing vector at $y = B_1$ $\overrightarrow{n}_1 = \langle -B_{1x}, 1\rangle$, and $\overrightarrow{n}_2 = -\langle -B_{2x}, 1\rangle$ the normal vector at $y = B_2$.

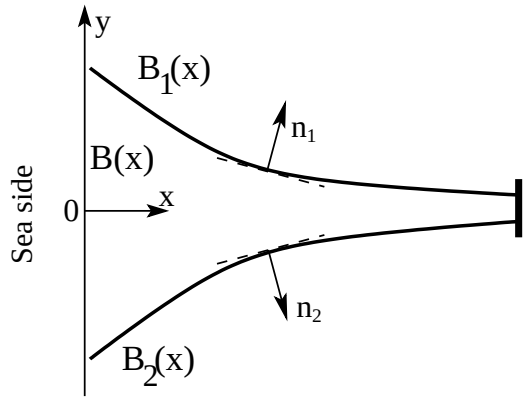

Fig. S.1 Sketch of the top view of the model geometry. A Cartesian coordinate system is used, the x axis is along-channel coordinate directed landwards and y axis is transverse coordinate points upwards.

Using the boundary condition (S.4), terms 1 and 2 in Eq. (S.3) drop out and the equation reduces to

$$\frac{\partial}{\partial t}\int_{B_2}^{B_1} c dy + \frac{\partial}{\partial x}\int_{B_2}^{B_1} ucdy + \frac{\partial}{\partial z}\int_{B_2}^{B_1} c(w-w_s)dy - \frac{\partial}{\partial x}\int_{B_2}^{B_1} K_h c_x dy - \frac{\partial}{\partial z}\int_{B_2}^{B_1} K_v c_z dy = 0. \tag{S.5}$$

Next write the concentration $c = \hat{c} + c'$, with $\hat{c}$ the width-averaged concentration, defined as

$$\hat{c} = \frac{1}{B(x)}\int_{B_2}^{B_1} c dy,$$

and c' fluctuations in the y-direction, defined as $c' = c - \hat{c}$. Here $B(x) = B_1(x) - B_2(x)$ is the width of the estuary. Similarly write $u = \hat{u} + u'$. Using the Leibniz integral rule, the width-integrated sediment concentration equation (S.5) reads

$$(B\hat{c})_t + (B\hat{u}\hat{c})_x + (B\hat{c}(\hat{w}-w_s))_z - (K_h B\hat{c}_x)_x - (K_v B\hat{c}_z)_z = 0, \tag{S.6}$$

where we assumed that the sediment concentration at the transversal boundaries equals the width-averaged concentration, i.e. $c\big|_{y=B_1} = c\big|_{y=B_2} = \hat{c}$. Moreover, we assume that correlations $\frac{\partial}{\partial x}\int_{B_2}^{B_1} u'c'dy$ can be modeled as a dispersive contribution.

Finally, using continuity equation (2a) and assuming that the width of the estuary is exponentially converging ($B(x) = B_0 e^{-x/L_b}$), the width-averaged concentration equation (S.6) reduces to

$$\hat{c}_t + \hat{u}\hat{c}_x + \hat{c}_z(\hat{w}-w_s) = (K_h\hat{c}_x)_x + (K_v\hat{c}_z)_z - \frac{1}{L_b}K_h\hat{c}_x. \tag{S.7}$$

This is expression (8) in the main text, where the hats ($\wedge$) have been dropped for simplicity.

S2 Morphodynamic equilibrium condition

The time evolution equation for the bed (Van Rijn, 1993) reads

$$\rho_s(1-p)\frac{\partial z_b}{\partial t} = D - E_s, \tag{S.8}$$

with ρ_s the density and p the porosity of the sediment. The depositional sediment flux D normal to the bottom is given by

$$D = B\hat{D} \equiv B(w_s\hat{c}n_z) \quad \text{at} \quad z=-H, \tag{S.9}$$

and the $3D$ erosional sediment flux reads $E_s = -K_h\overrightarrow{\nabla}c - K_v\frac{\partial c}{\partial z}\overrightarrow{n}_z$. By integrating this equation over the width, neglecting the transversal bottom variations and assuming that the concentration at the transversal boundaries equals the width-averaged concentration, i.e. $c\big|_{y=B_1} = c\big|_{y=B_2} = \hat{c}$, we obtain the width-averaged erosional sediment flux

$$\hat{E}_s = -K_h\hat{c}_x n_x - K_v\hat{c}_z n_z \quad \text{at} \quad z=-H. \tag{S.10}$$

with $n_x = H_x/|\overrightarrow{n}|$ and $n_z = 1/|\overrightarrow{n}|$ the components of the unit normal vector $\overrightarrow{n}$ at the bottom.

A relation between deposition and erosion is derived from the sediment concentration equation (S.6) by integrating it over the depth and using the Leibniz integral rule

$$\begin{aligned}
&\frac{\partial}{\partial t}\int_{-H}^{\zeta} B\hat{c}dz + \frac{\partial}{\partial x}\int_{-H}^{\zeta} B\hat{u}\hat{c}dz - \frac{\partial}{\partial x}\int_{-H}^{\zeta} K_h B\hat{c}_x dz = \\
&-B\underbrace{(w_s\hat{c} + K_h\hat{c}_x H_x + K_v\hat{c}_z)_{z=-H}}_{I} + B\hat{c}\underbrace{(\zeta_t + \hat{u} - \hat{w})_{z=\zeta}}_{II} + \\
&B\hat{c}\underbrace{(\hat{u}H_x + \hat{w})_{z=-H}}_{III} + B\underbrace{(w_s\hat{c} - K_h\hat{c}_x\zeta_x + K_v\hat{c}_z)_{z=\zeta}}_{IV}
\end{aligned} \tag{S.11}$$

Terms II, III, IV are eliminated due to boundary conditions (4), (5) and (9), i.e.,

$$\hat{w} = \zeta_t + \hat{u}\zeta_x \qquad \text{at} \quad z=\zeta, \tag{S.12a}$$

$$\hat{w} = -\hat{u}H_x \qquad \text{at} \quad z=-H, \tag{S.12b}$$

$$-w_s\hat{c} - K_v\hat{c}_z + K_h\hat{c}_x\zeta_x = 0 \qquad \text{at} \quad z=\zeta, \tag{S.12c}$$

and term I, according to Eqs. (S.9) and (S.10), can be expressed as $-B(D-E_s)$. Therefore, Eq. (S.11) reduces to

$$\begin{aligned}
&\frac{\partial}{\partial t}\int_{-H}^{\zeta} B\hat{c}dz + \frac{\partial}{\partial x}\int_{-H}^{\zeta} B\hat{u}\hat{c}dz - \frac{\partial}{\partial x}\int_{-H}^{\zeta} BK_h\hat{c}_x dz = \\
&\qquad\qquad B(-D+E_s).
\end{aligned} \tag{S.13}$$

Next, we average the result over a tidal period and require that the bed does not change over a tidal period. This means that there is a tidally averaged balance between erosion and deposition, i.e. $\langle D\rangle - \langle E_s\rangle = 0$. Using this in Eq. (S.13) gives that

$$\left\langle \frac{\partial}{\partial x}\int_{-H}^{\zeta} B\hat{u}\hat{c}dz \right\rangle - \left\langle \frac{\partial}{\partial x}\int_{-H}^{\zeta} BK_h\hat{c}_x dz \right\rangle = 0. \tag{S.14}$$

The morphodynamic equilibrium condition is obtained by integrating Eq. (S.14) with respect to x:

$$\left\langle \int_{-H}^{\zeta} (\hat{u}\hat{c} - K_h\hat{c}_x)\,dz \right\rangle = 0. \tag{S.15}$$

The integration constant is set to zero as we require no mean sediment flux at the weir.

Eq. (S.15) is expression (12) in the main text, where the hats ($\wedge$) are dropped for simplicity.

S3 Perturbation analysis and solutions

This supplement is an extension of Section 3. As a first step, the variables are scaled by their typical order, see Table S.1. Note, contrary to the previous sections, u, w, ζ and c are the width-averaged quantities. The hats ($\wedge$) are dropped for simplicity. In Table S.1 dimensionless variables are denoted by a tilde ($\sim$). Apart from the velocity scale $U = \sigma A_{M_2}\ell/H_0$, a second along-channel velocity scale in the model is the typical velocity scale for the density driven residual circulation $U_d = gH_0\beta S_x/\sigma$.

Substituting the scaled variables into Eqs. (2a) and (2b) yields the dimensionless shallow water equations

$$\widetilde{u}_{\tilde{x}} + \widetilde{w}_{\tilde{z}} - \frac{\ell}{L_b}\widetilde{u} = 0, \tag{S.16a}$$

$$\begin{aligned}
&\widetilde{u}_{\tilde{t}} + \frac{U}{\sigma\ell}(\widetilde{u}\widetilde{u}_{\tilde{x}} + \widetilde{w}\widetilde{u}_{\tilde{z}}) + \lambda^{-2}\widetilde{\zeta}_{\tilde{x}} - \\
&\qquad\qquad \frac{U_d}{U}\widetilde{<s>_x}\left(\tilde{z} - \frac{A_{M_2}}{H_0}\widetilde{\zeta}\right) = \left(\frac{A_v}{\sigma H_0^2}\widetilde{u}_{\tilde{z}}\right)_{\tilde{z}},
\end{aligned} \tag{S.16b}$$

where $\lambda = \ell/L_w$ is the ratio of the convergence length or embayment length (depending on which one is smaller) and the frictionless tidal wavelength L_w. Eq. (3) has been used to obtain Eq. (S.16b).

The dimensionless boundary condition at the entrance is given by

$$\widetilde{\zeta} = \cos\widetilde{t} + \frac{A_{M_4}}{A_{M_2}}\cos(2\widetilde{t} - \phi) \quad \text{at} \quad \widetilde{x} = 0,$$

Table S.1 Scaling of physical variables.

	Scaling		
Physical Quantity	Typical Scale	Symbol	Variable
Time	M_2 tidal frequency	σ	$t=\sigma^{-1}\widetilde{t}$
Sea surface elevation	M_2 tidal amplitude	A_{M_2}	$\zeta=A_{M_2}\widetilde{\zeta}$
Vertical coordinate	Water depth at the entrance	H_0	$z=H_0\widetilde{z}$
Local water depth			$H=H_0\widetilde{H}$
Horizontal coordinate	Minimum of the estuary length or convergence length	ℓ	$x=\ell\widetilde{x}$
Horizontal velocity	Follows from the integration of the continuity equation (2a) over depth and requiring an approximate balance between the resulting contributions	$U=\frac{\sigma A_{M_2}\ell}{H_0}$	$u=U\widetilde{u}$
Vertical velocity	Obtained from the width-averaged continuity equation (2a) by requiring an approximate balance between the first and second term	$W=\frac{H_0}{\ell}U$	$w=W\widetilde{w}$
Sediment concentration	Typical magnitude of the quantity under consideration	$C=\frac{\rho_s A_v U a_*}{H_0 g' d_s}$	$c=C\widetilde{c}$
Salinity gradient		S_x	$<s>_x=S_x\widetilde{<s>}_x$
Erosion coefficient		a_*	$a=a_*\widetilde{a}$

where A_{M_4} is the amplitude of the M_4 tidal constituent. At the riverine side we find that

$$\int_{-\widetilde{H}}^{\varepsilon\widetilde{\zeta}}\widetilde{u}d\widetilde{z}=\frac{Q}{UH_0B}\quad\text{at}\quad\widetilde{x}=1,$$

with Q being the river discharge.

At the free surface $\widetilde{z}=\varepsilon\widetilde{\zeta}$ the boundary conditions read

$$A_v\widetilde{u}_{\widetilde{z}}=0\quad\text{and}\quad\widetilde{w}=\widetilde{\zeta}_{\widetilde{t}}+\frac{A_{M_2}}{H_0}\widetilde{u}\widetilde{\zeta}_{\widetilde{x}},$$

at the bottom $\widetilde{z}=-\widetilde{H}$ they are given by

$$\widetilde{w}=-\widetilde{u}\widetilde{H}_{\widetilde{x}}\quad\text{and}\quad\widetilde{u}_{\widetilde{z}}=\frac{sH_0}{A_v}\widetilde{u}.$$

The dimensionless sediment mass balance equation, obtained from Eq. (S.7), reads

$$\widetilde{c}_{\widetilde{t}}+\frac{U}{\sigma\ell}(\widetilde{u}\widetilde{c}_{\widetilde{x}}+\widetilde{w}\widetilde{c}_{\widetilde{z}})-\frac{w_s}{\sigma H_0}\widetilde{c}_{\widetilde{z}}-\frac{K_h}{\sigma\ell^2}\widetilde{c}_{\widetilde{x}\widetilde{x}}-\frac{K_v}{\sigma H_0^2}\widetilde{c}_{\widetilde{z}\widetilde{z}}-\frac{K_h}{\sigma\ell L_b}\widetilde{c}_{\widetilde{x}}=0. \tag{S.17}$$

The dimensionless boundary conditions for the suspended sediment concentration are given by

$$\frac{w_s}{\sigma H_0}\widetilde{c}+\frac{K_v}{\sigma H_0^2}\widetilde{c}_{\widetilde{z}}-\frac{K_hA_{M_2}}{\sigma\ell^2H_0}\widetilde{c}_{\widetilde{x}}\widetilde{\zeta}_{\widetilde{x}}\quad\text{at}\quad\widetilde{z}=\varepsilon\widetilde{\zeta},$$

and

$$-\frac{K_v}{\sigma H_0^2}\widetilde{c}_{\widetilde{z}}-\frac{K_h}{\sigma\ell^2}\widetilde{c}_{\widetilde{x}}\widetilde{H}_{\widetilde{x}}=\frac{w_s}{\sigma H_0}|\widetilde{u}_{\widetilde{z}}|\widetilde{a}\quad\text{at}\quad\widetilde{z}=-\widetilde{H}.$$

The dimensionless morphodynamic equilibrium condition (12) and integral condition (14) read

$$\left\langle\int_{-\widetilde{H}}^{\varepsilon\widetilde{\zeta}}(\widetilde{u}\widetilde{c}-\frac{K_h}{\ell U}\widetilde{c}_{\widetilde{x}})d\widetilde{z}\right\rangle=0, \tag{S.18}$$

and

$$\frac{\int_0^1\widetilde{a}e^{-\frac{\ell}{L_b}\widetilde{x}}d\widetilde{x}}{\int_0^1e^{-\frac{\ell}{L_b}\widetilde{x}}d\widetilde{x}}=1.$$

From observations, it usually follows that the ratio of the M_2 tidal amplitude A_{M_2} and undisturbed water depth H_0 is a small parameter, i.e. $\varepsilon=A_{M_2}/H_0\ll1$. In order to construct a solution of the system of equations as a perturbation series, we have to relate the order of magnitude of most non dimensional coefficients in the equations above to ε. These parameters, their order and actual magnitude are provided in Table S.2.

Table S.2 Order of magnitude of dimensionless parameters and their actual value

Nondimentional parameter	Order	Value	
		1980	2005
$\varepsilon\equiv A_{M_2}/H$	$\mathcal{O}(\varepsilon)$	0.14	0.13
$U/\sigma\ell$	$\mathcal{O}(\varepsilon)$	0.14	0.13
ℓ/L_b	$\mathcal{O}(1)$	1	
U_d/U	$\mathcal{O}(\varepsilon)$	0.27	0.29
$A_v/\sigma H_0^2=K_v/\sigma H_0^2$	$\mathcal{O}(1)$	1.57	0.86
$w_s/\sigma H_0$	$\mathcal{O}(1)$	$0.14-3.57$	
$K_h/\sigma\ell^2$	$\mathcal{O}(\varepsilon^3)$	7.9×10^{-4}	
$K_h/\sigma\ell L_b$	$\mathcal{O}(\varepsilon^3)$	7.9×10^{-4}	
A_{M_4}/A_{M_2}	$\mathcal{O}(\varepsilon)$	0.17	0.14
$K_h/\ell U$	$\mathcal{O}(\varepsilon^2)$	0.006	
$A_{M_2}K_h/\sigma\ell^2H_0$	$\mathcal{O}(\varepsilon^4)$	1.1×10^{-4}	

The dimensionless slip parameter sH_0/A_v is allowed to vary from zero (no slip) to a large value (full slip) in the model, its actual value is derived from observations. Moreover, we assume that Q/UH_0B is at most of order ε.

We approximate the solution of the dimensionless Eqs. (S.16), (S.17) and (S.18) together with the appropriate boundary conditions by expanding the physical variables in power series of the small parameter ε

$$\tilde{u} = \tilde{u}^0 + \varepsilon^1\tilde{u}^1 + \varepsilon^2\tilde{u}^2 + \dots$$
$$\tilde{w} = \tilde{w}^0 + \varepsilon^1\tilde{w}^1 + \varepsilon^2\tilde{w}^2 + \dots$$
$$\tilde{\zeta} = \tilde{\zeta}^0 + \varepsilon^1\tilde{\zeta}^1 + \varepsilon^2\tilde{\zeta}^2 + \dots$$
$$\tilde{c} = \tilde{c}^0 + \varepsilon^1\tilde{c}^1 + \varepsilon^2\tilde{c}^2 + \dots$$

where superscripts denote the order of ε. After substitution of these expansions in the equations and boundary conditions and collecting terms of equal powers of ε, one can investigate the dynamics of the system at different orders. The resulting reduced systems of the water motion and concentration equations and the morphodynamic equilibrium condition are given in Sections S3.1, S3.2 and S3.3, respectively.

S3.1 Leading order system of equations

In leading order, i.e. $\mathcal{O}(\varepsilon^0)$, the dimensional system of equations describing the water motion reads

$$u_x^{02} + w_z^{02} - \frac{u^{02}}{L_b} = 0, \tag{S.19a}$$
$$u_t^{02} + g\zeta_x^{02} - (A_v u_z^{02})_z = 0, \tag{S.19b}$$

where the first superscript denotes the order of ε. The second superscript indicates the frequency of the constituent under consideration, by using the index of the lunar frequency.

The boundary conditions at the riverine side requires the depth-averaged velocity to be zero at the weir and at the entrance the system is forced by the externally prescribed semi-diurnal tide. These conditions read

$$\zeta^{02} = A_{M_2}\cos(\sigma t) \quad \text{at} \quad x = 0, \tag{S.20a}$$
$$\int_{-H}^{0} u^{02}dz = 0 \quad \text{at} \quad x = L. \tag{S.20b}$$

At the free surface $z = 0$ the boundary conditions are given by

$$w^{02} = \zeta_t^{02}, \tag{S.21a}$$
$$A_v u_z^{02} = 0. \tag{S.21b}$$

At the bottom $z = -H(x)$ the boundary conditions read

$$w^{02} = -u^{02}\frac{\partial H}{\partial x}, \tag{S.22a}$$
$$A_v u_z^{02} = s u^{02}. \tag{S.22b}$$

The dynamics of the sediment concentration in leading order is given by

$$c_t^0 - w_s c_z^0 = (K_v c_z^0)_z. \tag{S.23}$$

Hence in leading order the evolution of the sediment concentration is governed by local inertia, settling and vertical mixing of sediments.

The boundary condition at the free surface $z = 0$ imposes a no flux condition through the boundary,

$$w_s c^0 + K_v c_z^0 = 0. \tag{S.24}$$

At the bottom, $z = -H(x)$, the boundary condition reads

$$-K_v c_z^0 = w_s \rho_s \frac{s|u^{02}(t,x)|}{g' d_s} a(x). \tag{S.25}$$

Since the water motion only consists of an M_2 tidal signal in leading order, it follows that the concentration has a residual component and all constituents with frequencies that are an even multiple of the M_2 tidal frequency, hence

$$c^0 = c^{00} + c^{04} + \dots. \tag{S.26}$$

The sediment concentration c^0 still depends on the unknown erosion coefficient $a(x)$.

Solution. The leading order equations for the water motion (S.19) and sediment concentration (S.23) allow solutions of the following form:

$$(u^{02}, w^{02}, \zeta^{02}) = \Re\left\{\left(\hat{u}^{02}(x,z), \hat{w}^{02}(x,z), \hat{\zeta}^{02}(x)\right)e^{i\sigma t}\right\}, \tag{S.27}$$
$$c^0 = c^{00}(x,z) + \Re\left\{\hat{c}^{04}(x,z)e^{2i\sigma t} + \dots\right\}, \tag{S.28}$$

where $\Re\{.\}$ denotes the real part of the expression in braces and i is the imaginary unit.

To solve for the water motion, substitute (S.27) in Eqs. (S.19). This results in a system of ordinary differential equations for the spatial variables $\hat{u}^{02}(x,z)$, $\hat{w}^{02}(x,z)$ and $\hat{\zeta}^{02}(x)$

$$\hat{u}_x^{02} + \hat{w}_z^{02} - \frac{\hat{u}^{02}}{L_b} = 0, \tag{S.29a}$$
$$i\sigma\hat{u}^{02} + g\hat{\zeta}_x^{02} - (A_v\hat{u}_z^{02})_z = 0. \tag{S.29b}$$

First, momentum equation (S.29b) is solved using the corresponding boundary conditions for $\hat{u}^{02}$ at $z = 0$ and $z = -H(x)$. The resulting expression for $\hat{u}^{02}$ still depends on the unknown sea surface elevation $\hat{\zeta}^{02}$ and reads

$$\hat{u}^{02} = -\frac{g\hat{\zeta}_x^{02}}{i\sigma}\left(1 - \alpha(x)\cosh(\beta(x)z)\right), \tag{S.30}$$

here $\alpha = s/\left(A_v\beta\sinh(\beta H) + s\cosh(\beta H)\right)$ and $\beta = \sqrt{i\sigma/A_v}$.

Next, the continuity equation (S.29a) is used to solve for $\hat{w}^{02}$. The boundary condition for $\hat{w}^{02}$ at $z=0$ is satisfied using the integration constant. This results in

$$w^{02} = \frac{g}{i\sigma}\left(\frac{\zeta_x^{02}}{L_b} - \zeta_{xx}^{02}\right)\left(z - \frac{\alpha}{\beta}\sinh(\beta z)\right) + \frac{g\sinh(\beta z)\zeta_x^{02}}{i\sigma\beta}\left(\alpha_x + \alpha\beta_x\left(z\coth(\beta z) - \frac{1}{\beta}\right)\right) - i\sigma\zeta^{02},$$

To satisfy the other boundary condition (S.22a), an ordinary differential equation for $\hat{\zeta}^{02}$ has to be solved, usually numerically. This equation reads

$$T_1\hat{\zeta}_{xx}^{02} - T_2\hat{\zeta}_x^{02} - T_3\hat{\zeta}^{02} = 0,$$

with

$$T_1 = \frac{\alpha\sinh(\beta H)}{\beta} - H,$$

$$T_2 = \frac{T_1}{Lb} - \frac{\alpha_x\sinh(\beta H)}{\beta} + H_x(1-\alpha\cosh(\beta H)) + \frac{\alpha\beta_x(\sinh(\beta H) - \beta H\cosh(\beta H))}{\beta^2},$$

$$T_3 = \frac{\sigma^2}{g}.$$

By back-substituting $\hat{\zeta}^{02}$, we obtain the spatial velocities $\hat{u}^{02}$ and $\hat{w}^{02}$.

Next, we solve the sediment concentration equation (S.23) using substitution (S.28). Because Eq. (S.28) is linear, we can construct and solve an ordinary differential equation with respect to each spatial component (i.e. c^{00}, $\hat{c}^{04}$, etc) of the leading order concentration c^0 separately. As follows from Section S3.3, we only require the spatial variables c^{00} and $\hat{c}^{04}$ to calculate the equilibrium sediment distribution. The solution for these components reads

$$c^{00} = \frac{a(x)\rho_s s a_0}{g' d_s} e^{\frac{-w_s(H+z)}{K_v}},$$

$$\hat{c}^{04} = a(x)\left(A_1 e^{\frac{(\lambda-w_s)z}{2K_v}} + A_2 e^{\frac{-(\lambda+w_s)z}{2K_v}}\right), \tag{S.31}$$

with $\lambda = \sqrt{w_s^2 + 8i\sigma K_v}$, A_1 and A_2 are the integration constants, obtained from boundary conditions (S.24) and (S.25)

$$A_2 = \frac{-2w_s\rho_s s(a_2 - ib_2)(w_s+\lambda)}{g' d_s\left((\lambda - w_s)^2 e^{\frac{(w_s-\lambda)H}{2K_v}} - (w_s+\lambda)^2 e^{\frac{(w_s+\lambda)H}{2K_v}}\right)},$$

$$A_1 = -\frac{A_2(w_s-\lambda)}{w_s+\lambda}.$$

and a_0, a_2 and b_2 are coefficients of the Fourier series of the absolute value of the M_2 tidal velocity at the bed

$$|\hat{u}^{02}(x,-H)| = a_0 + a_1\cos(\sigma t) + b_1\sin(\sigma t) + a_2\cos(2\sigma t) + b_2\sin(2\sigma t) + \cdots$$

S3.2 First order system of equations

In this section the first order system of equations is given. The water motion is discussed in subsection S3.2.1 and sediment dynamics in S3.2.2.

S3.2.1 Water motion

The first order dimensional hydrodynamic equations, i.e. $\mathcal{O}(\varepsilon^1)$ is given by

$$u_x^1 + w_z^1 - \frac{u^1}{L_b} = 0, \tag{S.32a}$$

$$u_t^1 + u^{02}u_x^{02} + w^{02}u_x^{02} + g\zeta_x^1 - g\beta\,\langle s\rangle_x z = (A_v u_z^1)_z. \tag{S.32b}$$

At this order the advective contributions enter the momentum equation (S.32b).

At the free surface $z=0$ the boundary conditions read

$$w^1 = \zeta_t^1 - \zeta^{02}w_z^{02} + u^{02}\zeta_x^{02}, \tag{S.33a}$$

$$A_v u_z^1 + A_v\zeta^{02}u_{zz}^{02} = 0, \tag{S.33b}$$

and at the bottom $z=-H(x)$

$$w^1 = -u^1\frac{\partial H}{\partial x}, \tag{S.34a}$$

$$A_v u_z^1 = s u^1. \tag{S.34b}$$

The boundary conditions at the riverine side and entrance are given by

$$\zeta^1 = A_{M_4}\cos(2\sigma t - \phi) \quad \text{at} \quad x=0, \tag{S.35}$$

$$\int_{-H}^{0} u^1 dz + \frac{H_0}{A_{M_2}}u^{02}\Big|_{z=0}\zeta^{02} = \frac{Q}{B} \quad \text{at} \quad x=L. \tag{S.36}$$

From Eq. (S.30) and boundary condition (S.20b) we can conclude that $u^{02}=0$ at $x=L$. Therefore, boundary condition (S.36) reduces to

$$\int_{-H}^{0} u^1 dz = \frac{Q}{B} \quad \text{at} \quad x=L.$$

Careful inspection of the higher-order system of equations and the boundary conditions shows that the order ε velocity fields u^1, w^1 and the sea surface elevation ζ^1 consist of the residual contributions $(u^{10}, w^{10}, \zeta^{10})$ and contributions $(u^{14}, w^{14}, \zeta^{14})$ with twice the frequency of the semi-diurnal tide. Hence, the solution of the first order water motion can be expressed as, e.g. $u^1 = u^{10} + u^{14}$.

Residual flow. By averaging over a tidal period, a forced linear system that describe the residual flow is obtained

$$u_x^{10} + w_z^{10} - \frac{u^{10}}{L_b} = 0, \tag{S.37a}$$

$$\left\langle u^{02}u_x^{02} + w^{02}u_x^{02}\right\rangle + g\zeta_x^{10} - g\beta\,\langle s\rangle_x z = (A_v u_z^{10})_z, \tag{S.37b}$$

where the angular brackets $< . >$ denote a tidal average.

At the free surface $z = 0$ the boundary conditions are given by

$$w^{10} = -\left\langle \zeta^{02} w_z^{02} - u^{02}\zeta_x^{02} \right\rangle, \tag{S.38a}$$

$$A_v u_z^{10} + \left\langle A_v \zeta^{02} u_{zz}^{02} \right\rangle = 0. \tag{S.38b}$$

At the bottom $z = -H(x)$ the boundary conditions read

$$w^{10} = -u^{10}\frac{\partial H}{\partial x}, \tag{S.39a}$$

$$A_v u_z^{10} = s u^{10}. \tag{S.39b}$$

The boundary condition at the riverine side is that the depth- and tidally-averaged velocity is related to the river discharge at the weir by

$$\int_{-H}^{0} u^{10} dz dt = \frac{Q}{B} \quad \text{at} \quad x = L. \tag{S.40}$$

Furthermore, the residual sea surface elevation is zero at the entrance

$$\zeta^{10} = 0 \quad \text{at} \quad x = 0. \tag{S.41}$$

First overtide (M_4) flow. The M_4 constituent of the water motion is described by the following system of forced equations

$$u_x^{14} + w_z^{14} - \frac{u^{14}}{L_b} = 0, \tag{S.42a}$$

$$u_t^{14} + \left[u^{02}u_x^{02} + w^{02}u_x^{02}\right] + g\zeta_x^{14} = (A_v u_z^{14})_z, \tag{S.42b}$$

where braces $[.]$ denote the M_4 contribution.
At the free surface $z = 0$ the boundary conditions are given by

$$w^{14} = \zeta_t^{14} + [u^{02}\zeta_x^{02} - \zeta^{02} w_z^{02}], \tag{S.43a}$$

$$A_v u_z^{14} + A_v[\zeta^{02} u_{zz}^{02}] = 0. \tag{S.43b}$$

At the bottom $z = -H(x)$ the boundary conditions read

$$w^{14} = -u^{14}\frac{\partial H}{\partial x}, \tag{S.44a}$$

$$A_v u_z^{14} = s u^{14}. \tag{S.44b}$$

The first overtide boundary conditions at the entrance and riverine side are identical to those of the leading order conditions, but at the entrance the system is forced by the externally prescribed M_4 tide. These conditions are

$$\zeta^{14} = A_{M_4}\cos(2\sigma t - \phi) \quad \text{at} \quad x = 0, \tag{S.45a}$$

$$\int_{-H}^{0} u^{14} dz = 0 \quad \text{at} \quad x = L. \tag{S.45b}$$

The first order system of equations for the water motion consists of residual contributions, given by Eqs. (S.37)-(S.41), and M_4 contributions (Eqs. (S.42)-(S.45)). The residual and M_4 water motion is forced by various contributions, see the main text for a detailed description of these forcing terms.

Since the Eqs. (S.37) and boundary conditions (S.38)-(S.41) are linear, we can solve the equations for each forcing term separately. The solution method for each forcing term is similar to the method described in Section S3.1.

Similar to (S.27), the M_4 water motion equations (S.42) allow the solution of the following form

$$\left(u^{14}, w^{14}, \zeta^{14}\right) = \Re\left\{\left(\widetilde{u}^{14}(x,z), \widetilde{w}^{14}(x,z), \widetilde{\zeta}^{14}(x)\right) e^{2i\sigma t}\right\}, \tag{S.46}$$

here $\Re\{.\}$ stands for the real part of an expression in braces and i the imaginary unit. Substitution (S.46) in Eqs. (S.42) results in a system of ODEs with respect to the spatial variables $\widetilde{u}^{14}(x,z)$, $\widetilde{w}^{14}(x,z)$ and $\widetilde{\zeta}^{14}(x)$. The resulting system of equations is linear. Analogous to the method which was employed for the residual water motion, we decompose the system and boundary conditions into three systems of ODEs with appropriate boundary conditions each induced by the individual forcing. Next, we obtain the solution for each system and construct the final solution as a superposition $(\widetilde{u}^{14}, \widetilde{w}^{14}, \widetilde{\zeta}^{14}) = \sum_{i=1}^{3} (\widetilde{u}_i^{14}, \widetilde{w}_i^{14}, \widetilde{\zeta}_i^{14})$.

S3.2.2 Sediment dynamics

In deriving the sediment equation at first order, we assume that the nonlinear terms in Eq. (S.17) are negligible in the dynamics of the suspended sediment concentration, even though they give an order epsilon contribution according to the scaling. The motivation for this choice is that treating these nonlinear terms as order ε quantities will result in additional mean and overtide components of the first order. Solving these components will be straightforward, but will also complicate the analysis. Since our goal is to gain understanding of sediment transport, these nonlinear terms are neglected at a first step. Hence, the dynamics of the sediment concentration is governed by

$$c_t^1 - w_s c_z^1 = (K_v c_z^1)_z. \tag{S.47}$$

The first order boundary conditions for the sediment concentration are equivalent to those in leading order, with the first order component of the absolute value of the bed shear stress

$$|\tau_b^1| = \rho_0 s u^1 \frac{u^{02}}{|u^{02}|} \quad \text{at} \quad z = -H. \tag{S.48}$$

The boundary conditions read

$$w_s c^1 + K_v c^1_z = 0 \quad \text{at} \quad z = 0, \tag{S.49}$$

$$-K_v c^1_z = w_s \rho_s s u^1 \frac{u^{02}}{|u^{02}| g' d_s} a(x) \quad \text{at} \quad z = -H. \tag{S.50}$$

Hence, the first-order sediment concentration is a result of the leading order and the first order tidal flow interaction. Applying the Fourier analysis to bottom boundary condition (S.50), it can be deducted that the first order concentration consist of all tidal components

$$c^1 = c^{10} + c^{12} + \dots. \tag{S.51}$$

The semi-diurnal component of the first order sediment concentration c^{12} is obtained by substituting

$$c^{12} = \Re\left\{\hat{c}^{12}(x,z) e^{i\sigma t}\right\} \tag{S.52}$$

in concentration equation (S.47). This results in an ordinary differential equation for the spatial coefficient $\hat{c}^{12}(x,z)$. Using the appropriate boundary conditions (S.49) and (S.50) the solution to this equation reads

$$\hat{c}^{12} = a(x)\left(B_1 e^{\frac{(\lambda - w_s)z}{2K_v}} + B_2 e^{\frac{-(\lambda + w_s)z}{2K_v}}\right), \tag{S.53}$$

with $\lambda = \sqrt{w_s^2 + 4i\sigma K_v}$, B_1 and B_2 are the integration constants, obtained from boundary conditions (S.24) and (S.25)

$$B_2 = \frac{-2 w_s \rho_s s (p_1 - i d_1)(w_s + \lambda)}{g' d_s \left((\lambda - w_s)^2 e^{\frac{(w_s - \lambda)H}{2K_v}} - (w_s + \lambda)^2 e^{\frac{(w_s + \lambda)H}{2K_v}}\right)},$$

$$B_1 = -\frac{B_2 (w_s - \lambda)}{w_s + \lambda}.$$

and p_1 and d_1 are coefficients of the Fourier series of the absolute value of the bed shear stress given by Eq. (S.48)

$$\hat{u}^1(x,-H)\frac{\hat{u}^{02}(x,-H)}{|\hat{u}^{02}(x,-H)|} = p_0 + p_1\cos(\sigma t) + d_1 \sin(\sigma t) + p_2 \cos(2\sigma t) + d_2 \sin(2\sigma t) + \cdots$$

S3.3 Morphodynamic equilibrium condition

From the scaled morphodynamic equilibrium condition (S.18) and the fact that in leading order the concentration consists of a residual component and a component with a frequency that is multiple of M_4 (S.26) and velocity only of an M_2, it is evident that there is no residual sediment transport in order ε. Only in order ε^2 a residual sediment transport is found, due to the interaction of the residual and M_4 $\mathcal{O}(1)$ sediment concentration with the residual and M_4 $\mathcal{O}(\varepsilon)$ velocity components, and the M_2 $\mathcal{O}(\varepsilon)$ sediment concentration with the M_2 $\mathcal{O}(1)$ velocity component. The morphodynamic equilibrium condition reads

$$\int_{-H}^{0} (u^{10}c^{00} + \langle u^{02}c^{12}\rangle + \langle u^{14}c^{04}\rangle - K_h \langle c^{00}_x\rangle) dz + \underbrace{\langle \zeta^0 [u^0 c^0]_{z=0}\rangle}_{E} = 0. \tag{S.54}$$

Note that in Eq. (S.54) the last contribution (E) is a result of Taylor expansion the upper integration boundary in Eq. (S.18) around $z = 0$.

The spatial and temporal structure of the width-averaged sediment concentration c is known but it still depends on the unknown erosion coefficient $a(x)$, i.e. $c^{00} = a(x)c^{00a}$, $c^{04} = a(x)c^{04a}$ and $c^{12} = a(x)c^{12a}$ The spatial and temporal structure of the width-averaged velocity fields is known. Substituting these expressions in the morphodynamic equilibrium condition (S.54) results in a linear first order ODE with respect to the unknown erosion coefficient $a(x)$

$$F\frac{da}{dx} + Ta = 0, \tag{S.55}$$

where

$$F = \left\langle \int_{-H}^{0} -K_h c^{00a} dz \right\rangle,$$

$$T = \int_{-H}^{0} \left(u^{10}c^{00a} + \langle u^{02}c^{12a}\rangle + \langle u^{14}c^{04a}\rangle - K_h \langle c^{00a}_x\rangle\right) dz + \left\langle \zeta^0 \left[u^{02}c^{0a}\right]_{z=0}\right\rangle.$$

Eq. (S.55) is solved by the method of separation of variables. The solution reads

$$a(x) = a_0 exp\left(\int -T/F dx\right) \equiv a_0 I(x), \tag{S.56}$$

The integration constant is denoted by a_0 and determined from condition (14) as

$$a_0 = \frac{a_* \int_0^L B(x) dx}{\int_0^L B(x) I(x) dx}. \tag{S.57}$$

S4 Parameter sensitivity

This supplement is an extension of Section 5.1. In the supplement we investigate the physical mechanisms which are responsible for the amplification of the semi-diurnal tidal amplitude between 1980 and 2005. The M_2 tidal amplitude

and relative phase between the horizontal velocity and water level are shown in Fig. S.2 by the solid blue and green lines, respectively. Comparison of these lines suggests that the tidal motion is more resonant in 2005 than 1980: in 1980 the dimensionless M_2 sea surface elevation amplitude at the weir (the ratio of the M_2 sea surface elevation amplitude over its value at the entrance) was approximately 0.74, in 2005 1.12. Moreover, the relative phase (see Fig. S.2(b)) suggests more of a standing wave character in 2005 than in 1980.

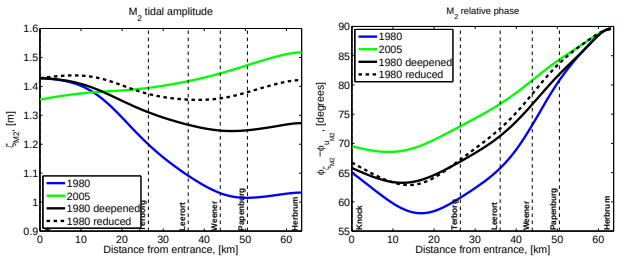

Fig. S.2 The semi-diurnal tidal amplitude and phase difference between the semi-diurnal horizontal velocity and water level. The left panels represent tidal amplitude along the estuary and the right ones depict relative phase shift between the free surface elevation and along-channel velocity component.

The two main differences in the model input between 1980 and 2005 are the depth of the embayment and the change of the vertical eddy viscosity parameter A_v and stress parameter s. As a first step, we want to understand whether these changes result from a combination of those two factors or are primarily caused by one of the factors, for example, deepening. Therefore, we consider deepening and change of parameters A_v and s separately and compare these results with those which are obtained for the 1980 and 2005 experiments. As a first experiment, we take the model setup for 1980 with a deepened bathymetry, but keeping the parameters of A_v and s unchanged. The resulting M_2 amplitude is shown by the black solid line in Fig. S.2(a), in Fig. S.2(b) the relative phase is shown. It is clear that the system has became more resonant as both the amplitude increases towards the end of the embayment and the relative phase has became closer to 90°. Next, we use the 1980 model setup with reduced values of A_v and s, but keeping the 1980 bathymetry. The M_2 amplitude is depicted by the black dashed line in Fig. S.2(a) and the relative phase is shown in Fig. S.2(b). This model input makes the M_2 amplitude increase even faster and gives higher value of the relative phase, compared to the previous model setup. Hence makes the system more resonant than by only deepening itself. However, we can conclude that it is the combination of deepening and reduced vertical eddy viscosity and stress parameter that makes the M_2 tide amplify towards the end of the estuary.

The M_4 tidal amplitude significantly amplifies towards the end of the embayment in 2005, the dimensionless M_2 sea surface elevation amplitude at the weir is 2.39, whereas in 1980 it's only 0.98 (the green and blue solid lines in Fig. S.3(a), respectively). The relative phase, shown in Fig. S.3(b), suggests more of a standing wave character in 2005. Repeating the above experiments, it turns out that for the M_4 tidal motion, it is mainly the reduction of the vertical viscosity and stress parameter (by the black dashed line in Fig. S.3(a)) that results in the amplification of the M_4 tidal amplitude. For the M_4 relative phase both the deepening and the reduction of the vertical viscosity and stress parameter are essential to reproduce the 2005 model results.

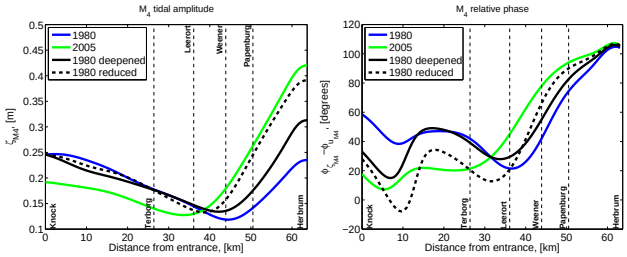

Fig. S.3 The M_4 tidal amplitude and phase difference between the M_4 horizontal and vertical tide. The left panels represent tidal amplitude along the estuary and the right ones depict relative phase shift between the free surface elevation and along-channel velocity component.

Because we use an analytical approach, we can split the M_4 tidal signal into a part generated due to nonlinear interactions in the model and a contribution due to the external overtide forcing. The amplitude and relative phase of the internally generated M_4 tide is shown in Fig. S.4 and for the externally forced M_4 tide in Fig. S.5. Based on Fig. S.4(a), we observe that the amplification of the internally generated M_4 tide is mainly achieved by a reduction of the bottom friction and vertical eddy viscosity parameters. The externally forced M_4 tide exhibits similar behavior as the M_2 tide.

To get more insight in the effect of the bottom friction and deepening on the resonance characteristics of the tidal embayment, we develop a simple analytical model of an estuary with a flat bed constrained by a weir. To this end we choose a representative water depth ($7.7m$, $8.7m$) for 1980 and 2005, respectively, such that the tidal character for the M_2 water motion is well-reproduced in the simplified model (compare Figs. S.2(a) and S.6(a)). We see that in both models the M_2 tide shows similar behavior. Therefore, we can assume that the flat bed resonance characteristics are similar to model with varying bathymetry.

The dimensionless M_2 tidal amplitude at the weir is plotted as a function of the embayment length scaled with a quarter wavelength of the frictionless tidal wave $L_g = \sqrt{gH/\sigma}$

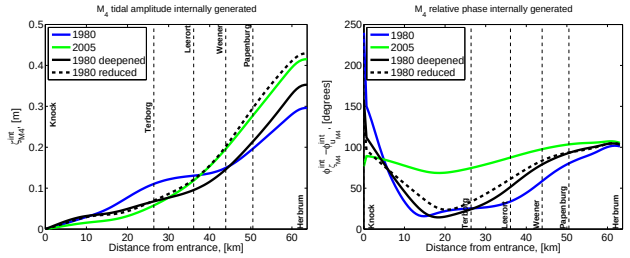

Fig. S.4 The M_4 internally generated tidal amplitude and phase difference between the M_4 horizontal and vertical tide internally generated. The left panels represent tidal amplitude along the estuary and the right ones depict relative phase shift between the free surface elevation and along-channel velocity component.

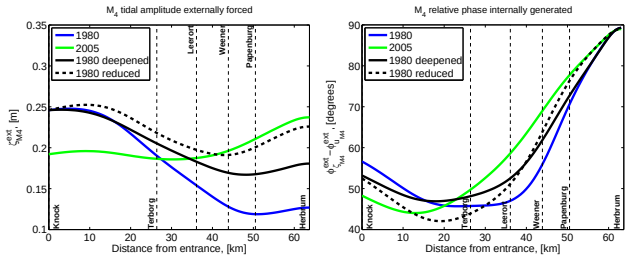

Fig. S.5 The M_4 externally forced tidal amplitude and phase difference between the M_4 horizontal and vertical tide externally forced. The left panels represent tidal amplitude along the estuary and the right ones depict relative phase shift between the free surface elevation and along-channel velocity component.

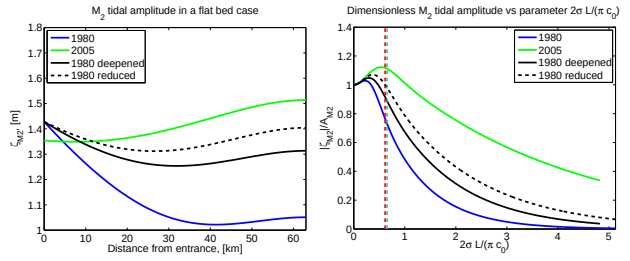

Fig. S.6 Flat bed model output. The left panel represent the M_2 tidal amplitude along the estuary and the right one depict the effect of bottom friction and deepening on the resonance characteristics.

in Fig. S.6(b). The vertical red dashed line represents the length of the embayment of $L = 63.7\ km$, which is the length of the Ems estuary, with depth $8.7m$ and the cyan dashed line $7.7m$. In 1980 the estuary is far from resonance, by either deepening or reducing the bottom friction and vertical eddy viscosity the embayment becomes more resonant. Decreasing the vertical eddy viscosity and friction parameter is slightly more efficient in pushing the embayment towards resonance than deepening. But, as it was already shown above, both deepening and decrease of the vertical eddy viscosity and stress parameter are necessary to reproduce the 2005 amplification. Hence, the combination of these factors enhances the resonance so that the M_2 tide, as well as M_4, amplifies even further towards the end of the estuary.

S5 Transport function components

This chapter is an extension of Section 5.2.1. In the next paragraphs we provide a detailed analysis of the transport function components T_{res}, T_{M_2} and T_{M_4}.

T_{M_2} **transport function**. The T_{M_2} contribution plays an important role in the changes of the sediment trapping location in the Ems estuary between 1980 and 2005. To understand which mechanism is responsible for this significant change of T_{M_2}, T_{M_2} will be decomposed into different components. The M_2 concentration (see Section 3.2.2), is forced by the M_2 component of the bed shear stress. From Eq. (36) it follows that the M_2 component of the bed shear stress is a result of the interaction of both the residual and the M_4 velocities with the M_2 velocity. Using Section 3.2.1, we can distinguish 5 contributions to the M_2 concentration due to the residual flow (see Eq. (32)) and 4 due to the M_4 flow (see Eq. (37)), each resulting in a contribution to T_{M_2}, that can be studied separately.

The residual contribution to T_{M_2} driven by the gravitational circulation is denoted by $T^{\text{GC}}_{M_2}$, for river discharge by $T^{\text{RI}}_{M_2}$, $T^{\text{SD}}_{M_2}$ denotes the contribution due to Stokes drift, $T^{\text{SC}}_{M_2}$ due to surface contribution and $T^{\text{TS}}_{M_2}$ due to tidal stresses. The M_4 velocity components that contribute to T_{M_2} are advective contributions, denoted by $T^{\text{AC}}_{M_2}$, free surface contribution, denoted by $T^{\text{FS}}_{M_2}$, no-stress contribution, denoted by $T^{\text{NS}}_{M_2}$, and the M_4 external forcing, denoted by $T^{\text{EF}}_{M_2}$ (see Section 3.2.2). The sum of the residual and M_4 contributions is denoted by $T^{\text{res}}_{M_2}$ and $T^{M_4}_{M_2}$, respectively. Hence

$$T_{M_2} = \underbrace{T^{\text{GC}}_{M_2} + T^{\text{RI}}_{M_2} + T^{\text{SD}}_{M_2} + T^{\text{SC}}_{M_2} + T^{\text{TS}}_{M_2}}_{T^{\text{res}}_{M_2}} + \underbrace{T^{\text{AC}}_{M_2} + T^{\text{FS}}_{M_2} + T^{\text{NS}}_{M_2} + T^{\text{EF}}_{M_2}}_{T^{M_4}_{M_2}}.$$

In Fig. S.7 T_{M_2} and its components $T^{\text{res}}_{M_2}$, $T^{M_4}_{M_2}$ are shown by the dashed green, solid red and solid blue lines, respectively. For fine silt we can observe no significant change of the $T^{\text{res}}_{M_2}$ contribution between 1980 and 2005. Therefore, the change in T_{M_2} is determined by the $T^{M_4}_{M_2}$ contribution. The $T^{M_4}_{M_2}$ flux starts to decrease at approximately km 20 in 1980, whereas in 2005 it stays constant up to approximately km 50 and only then starts to decrease. For coarse silt we observe a similar behavior of the $T^{M_4}_{M_2}$ flux: a smooth decrease from the entrance in 1980 and in 2005 the decrease starts at 50

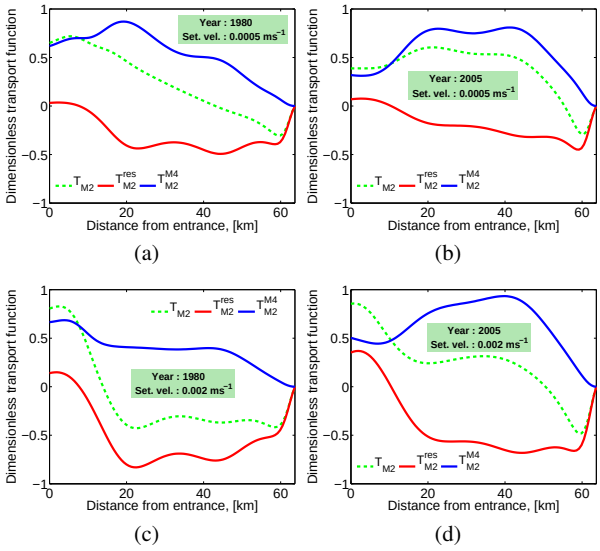

Fig. S.7 Dimensionless transport function T_{M_2} and its components.

km. For coarse silt, the magnitude of the $T^{\text{res}}_{M_2}$ flux has decreased between 1980 and 2005. However, the general behavior did not change. Hence, the change of T_{M_2} is again mainly caused by the change of its M_4 contribution. Therefore, further decomposition is needed to find the dominant difference between 1980 and 2005.

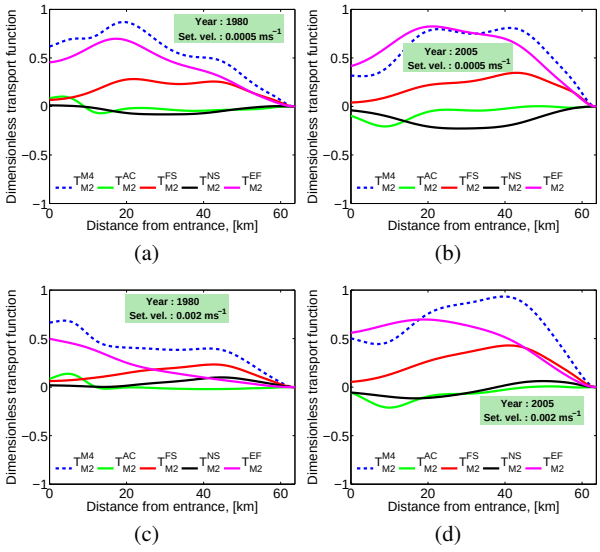

Fig. S.8 Dimensionless transport function $T^{M_4}_{M_2}$ and its components.

The M_4 components of the transport function T_{M_2} are shown in Fig. S.8. For both fine silt (Figs. S.8(a) and S.8(b)) and coarse silt (Figs. S.8(c) and S.8(d)), we see that the behavior of $T^{M_4}_{M_2}$ (the dashed blue line) is primarily determined by the contribution which results from the externally forced M_4 tide (the solid magenta line). The other three contributions are much smaller. It follows that for both years and grain sizes the main contribution to $T^{M_4}_{M_2}$ is the externally prescribed M_4 overtide. In 1980 this contribution decreases from the entrance, whereas in 2005 an abrupt decrease starts only at approximately *km* 40. Hence the main change between 1980 and 2005 is due to the difference in residual sediment transport by tidal asymmetry: there was less import of sediment in 1980 compared to 2005. This is true for both fine and coarser silt.

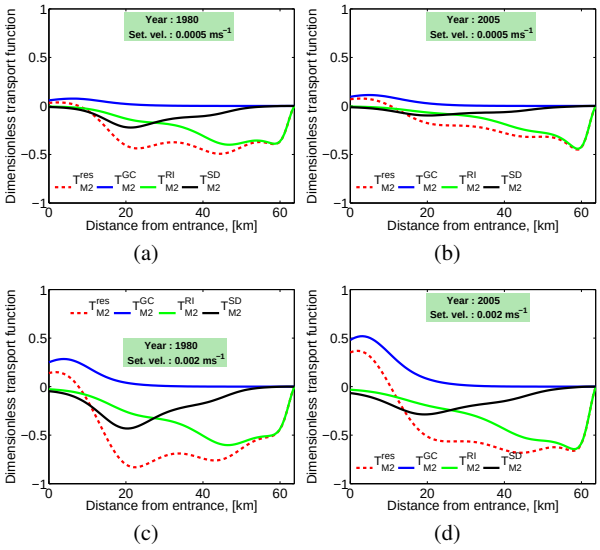

Fig. S.9 Dimensionless transport function $T^{\text{res}}_{M_2}$ and its components.

In Fig. S.9 a decomposition of $T^{\text{res}}_{M_2}$ (the dashed red line) is shown. Three residual constituents ($T^{\text{GC}}_{M_2}$, the solid blue line, $T^{\text{RI}}_{M_2}$, the solid green line and $T^{\text{SD}}_{M_2}$, the solid black line, respectively) are shown. The two remaining contributions ($T^{\text{SC}}_{M_2}, T^{\text{TS}}_{M_2}$) are insignificant and therefore not shown. For fine silt (Figs. S.9(a) and S.9(b)) we observe that a decrease of the $T^{\text{SD}}_{M_2}$ contribution between 1980 and 2005. Close inspection of Figs. S.9(c) and S.9(d) shows that, for coarse silt, the $T^{\text{res}}_{M_2}$ flux has changed due to the increase of the $T^{\text{GC}}_{M_2}$ contribution and the decrease of the $T^{\text{SD}}_{M_2}$ contribution between 1980 and 2005. This is caused by an increase of the gravitational circulation and weakening of the tidal return flow in 2005 (see discussion in Section 5.1).

T_{M_4} **transport function**. The T_{M_4} flux is the result of the M_4 velocity and M_4 concentration interaction. The M_4 velocity consists of four constituents (see Eq. (37)) and hence, the T_{M_4} flux has four different contributions, i.e.

$$T_{M_4} = T^{\text{AC}}_{M_4} + T^{\text{FS}}_{M_4} + T^{\text{NS}}_{M_4} + T^{\text{EF}}_{M_4}.$$

The T_{M_4} flux (the dashed black line) and its components are shown in Fig. S.10. For fine and coarse silt (Figs.S.10(a), S.10(b) and Figs.S.10(c), S.10(d), respectively) the main balance is between the $T^{\text{NS}}_{M_4}$ contribution (the solid blue line)

and the $T_{M_4}^{\mathrm{EF}}$ transport (the solid magenta line). For fine silt, none of the components shows more than a 5 % change of behavior between 1980 and 2005. For coarse silt we see that changes of the T_{M_4} flux are primarily caused by changes in the advective contribution $T_{M_4}^{\mathrm{AC}}$ (the solid green line) and the $T_{M_4}^{\mathrm{EF}}$ transport functions.

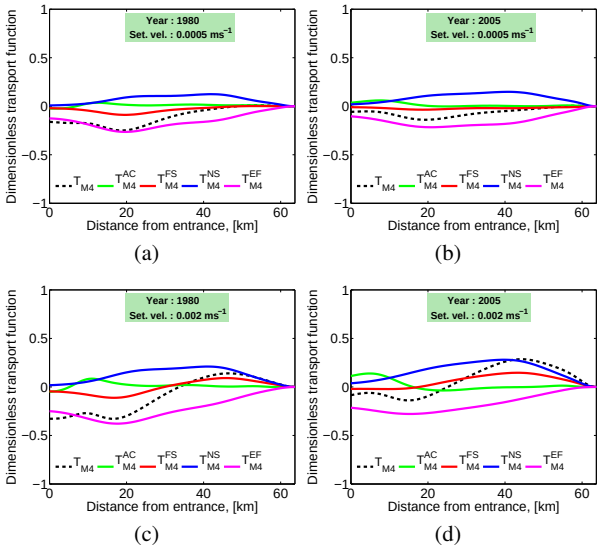

Fig. S.10 Dimensionless M_4 transport function in components.

T_{res} transport function. The T_{res} flux is a result of interactions of the residual velocity and residual concentration. The residual velocity consists of 5 constituents (see Eq. (32)). Hence, similar to the T_{M_2} transport function, the T_{res} flux can be decomposed in contributions forced by: the gravitational circulation $T_{\mathrm{res}}^{\mathrm{GC}}$, river inflow T_{res}^{RI}, tidal return flow $T_{\mathrm{res}}^{\mathrm{SD}}$, surface contribution $T_{\mathrm{res}}^{\mathrm{SC}}$, tidal stresses $T_{\mathrm{res}}^{\mathrm{TS}}$ and contribution $T_{\mathrm{res}}^{\zeta uc}$ resulting from a correlation between the tidal return flow and concentration

$$T_{\mathrm{res}} = T_{\mathrm{res}}^{\mathrm{GC}} + T_{\mathrm{res}}^{\mathrm{RI}} + T_{\mathrm{res}}^{\mathrm{SD}} + T_{\mathrm{res}}^{\mathrm{SC}} + T_{\mathrm{res}}^{\mathrm{TS}} + T_{\mathrm{res}}^{\zeta uc}.$$

Fig. S.11 shows the T_{res} flux (the dashed red line) and its 4 components: $T_{\mathrm{res}}^{\mathrm{GC}}$ (the solid blue line), $T_{\mathrm{res}}^{\mathrm{RI}}$ (the solid green line), $T_{\mathrm{res}}^{\mathrm{SD}}$ (the solid black line), $T_{\mathrm{res}}^{\zeta uc}$ (the solid magenta line). The other two contributions are not shown as they are negligible.

We can see that for both fine (Figs. S.11(a) and S.11(b)) and coarse silt (Figs. S.11(c) and S.11(d)) $T_{\mathrm{res}}^{\mathrm{SD}}$ is approximately balanced by the $T_{\mathrm{res}}^{\zeta uc}$ flux. Therefore, the behavior of the T_{res} flux is mainly determined by the river inflow flux $T_{\mathrm{res}}^{\mathrm{RI}}$ everywhere in the estuary, except in a region at the entrance. In this region we see the influence of the gravitation circulation flux $T_{\mathrm{res}}^{\mathrm{GC}}$.

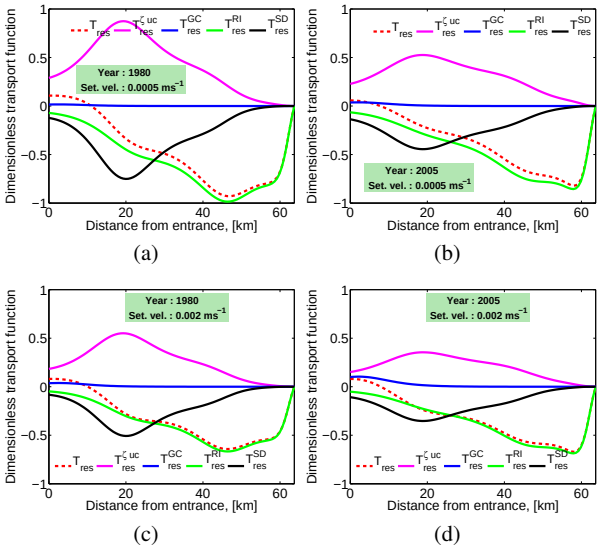

Fig. S.11 Dimensionless T_{res} transport function and its components.

References

Van Rijn LC (1993) Principles of sediment transport in rivers, estuaries and coastal seas. Aqua Publ., Amsterdam